Jean-Paul Ngoune, et. al. International Journal of Engineering Research and Applications
www.ijera.com
ISSN: 2248-9622, Vol. 14, Issue 5, May, 2024, pp: 19-26

RESEARCH ARTICLE OPEN ACCESS

Sliding Mode Direct Power Control of a DC-DC Bidirectional Converter for High Voltage Applications

Jean-Paul Ngoune*, Paul E. Owoundi**, Alexandre T. Boum**, Julius D. Cham**

**(Department of Electrical Engineering, ENSET, University of Douala, Douala, Cameroon*
Email: jngounepaul@gmail.com)
*** (Department of Electrical Engineering, ENSET, University of Douala, Douala, Cameroon)*

ABSTRACT
This paper proposes an efficient control scheme of a DC-DC bidirectional converter suitable for HV applications. The converter has an isolated topology. It comprises two 2-level parallel connected DC-AC converters at the left side of the isolation transformers and two series connected single phase 3-level neutral point clamped (NPC) converters at the right side. The interest of this structure is that it permits to generate a HV DC voltage using a lower DC voltage source and vice versa. The proposed scheme exploits both the advantages of sliding-mode control and direct power control, thus leading to accurate reference tracking, fast dynamic response, large-signal stability, and high robustness against line and load disturbance. A neutral point voltage balancing technique using an auxiliary inductive circuit is also proposed, with interesting performances. These results are obtained by simulations with Matlab-Simulink software.

Keywords **-** DC-DC bidirectional converter, 3-level NPC Converter, 2-level DC-AC converter, sliding mode direct power control, multilevel converters.

Date of Submission: 22-04-2024 Date of acceptance: 02-05-2024

I. INTRODUCTION

In these recent years static converters are more and more used in many applications such as household appliances, railway traction, maritime propulsion, heavy industry, aeronautics, just to name the few. Some of these applications require well regulated medium or high DC voltages [1]. These high voltages are difficult to obtain using classical DC-DC boost converters or 2-level AC-DC converters. In order to overcome these limitations, multilevel converters were developed, and many multilevel topologies created.

Multilevel converters are designed by series – parallel connection of already existing semiconductor switches. They permit to obtain more than 2 voltage levels at the output of the converter. The topology of the converter investigated in this paper was proposed by Prof. A. Rufer. It comprises two series connected single phase 3-level NPC converters at the right side, accompanied with two parallel connected 2-level inverters at the left side (Fig.1). NPC topologies are very suitable for medium power HV applications [2]. They have many interesting properties such as a reduced voltage stress on electronic switches, a reduced switching frequency leading to low switching losses; low total harmonic distortion for voltage signals, low electromagnetic interference levels; and a simple configuration [3-7]. The major challenge with NPC topologies is however the balancing of the voltages across capacitors at the DC side of the converter and the control of the neutral point voltage [8]. In the other hand DC-AC 2-level converters are also suitable for medium voltage applications [9]. Galvanic isolation featured by the converter we are studying, is one of the promising methods to achieve a high gain boost ability by adding an extra degree of freedom to the gain of the converter, namely the turn ratio of windings, and making it suitable for the HV applications. Apart from enabling a high voltage gain ratio, isolation has other benefits such as providing isolation between the input and output side, for the supply of sensitive loads [10].

The purpose of this work is therefore to provide a well regulated HVDC voltage supply using a lower DC voltage source. Given the bidirectional capability of the converter, it is also purposed to provide a well regulated LVDC supply using an HVDC source. This paper is organized as follows: In section 2, a study of the topology of the converter is carried out. Section 3 presents the proposed control technique. In section 4, simulation results are presented and discussed. Finally, the conclusion of the proposed work is addressed in Section 5.

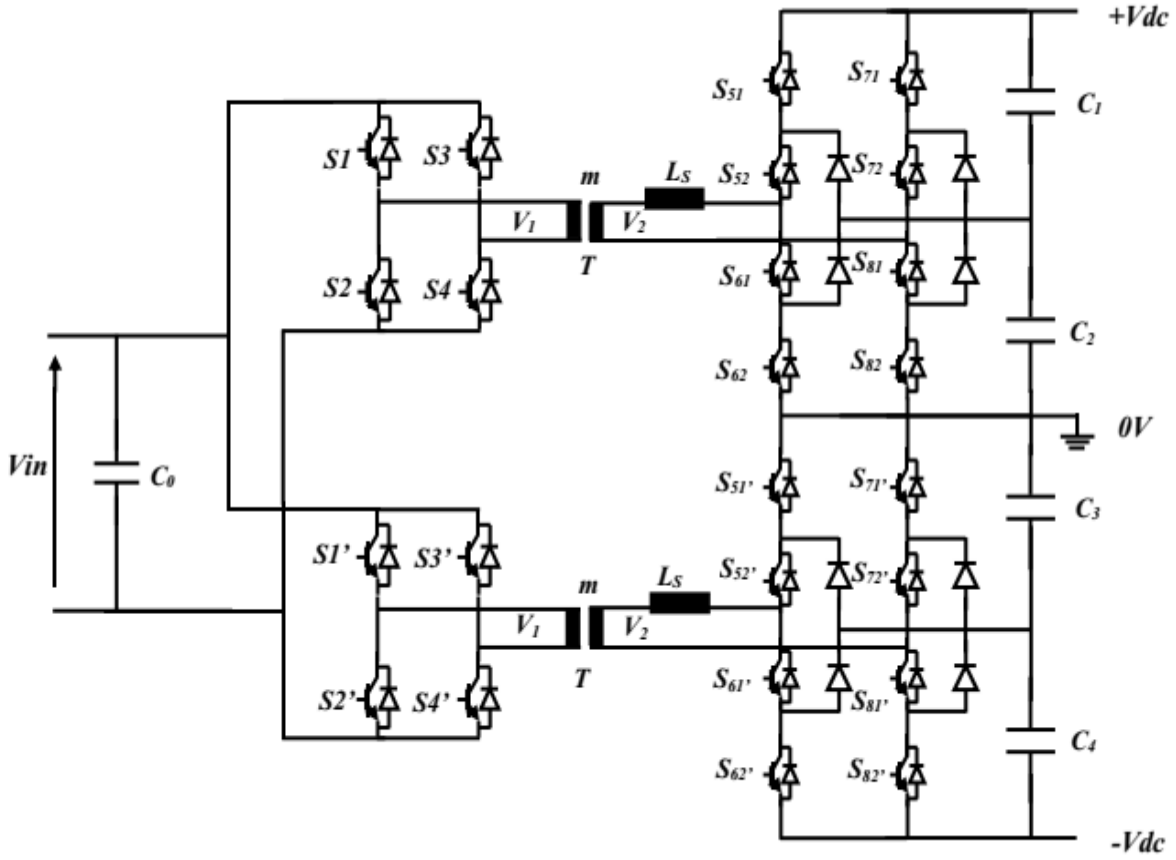

Fig. 1. Topology of the converter.

II. STUDY OF THE CONVERTER

The topology of the converter comprises two identical stages: an upper stage and a lower stage. We carry out the study of the upper stage only. This study can therefore be extended to the lower stage of the converter. Each stage is made of a single phase DC-AC converter at the left side of the isolation transformer and a single phase 3-level NPC AC-DC converter at the right side. The inductance *Ls* enables the power transfer from either side of the isolation transformer to the other side. This inductance introduces a phase shift γ between the voltage at the primary side of the transformer and the voltage at the secondary side; m is the transformation ratio. V_1 and V_2 are respectively the primary and the secondary voltages of the isolation transformer. Let f_s the switching frequency of the converter, the phase shift γ or phase difference time of the converter is defined as follows [11]:

$$\gamma = D \times T_S \quad (1)$$

$$D = \frac{T_{on}}{T_S} \quad (2)$$

And

$$T_s = \frac{1}{2f_s} \quad (3)$$

D is the duty ratio; T_S is the switching period, T_{on} is the duration of conduction of a switch in one cycle of functioning of the converter.

Each leg of the 3-level NPC converter has three possible switching states. Each switching state corresponds to one of the three voltage levels, as presented below (Table 1). However, given the fact that the transformer is fed by a 2-level DC-AC converter which provides only two voltage levels per cycle, we decide to eliminate one of the three switching states of the NPC converter, so that we have the same number of switching states for both

converters. We obviously eliminate the switching state N°2, which corresponds to the voltage $V_{AN} = 0$. Table 2 below presents the steady state operation of the converter on one cycle of its functioning *(1=ON; 0 =OFF).*

Table 1. Possible switching states in a leg of a 3 level NPC converter

Etat de commutation	**Bras du convertisseur NPC à trois niveaux**				**V_{AN}**
Switches	S1	S2	S3	S4	
1	1	1	0	0	*Vd/2*
2	0	1	1	0	*0*
3	0	0	1	1	*-Vd/2*

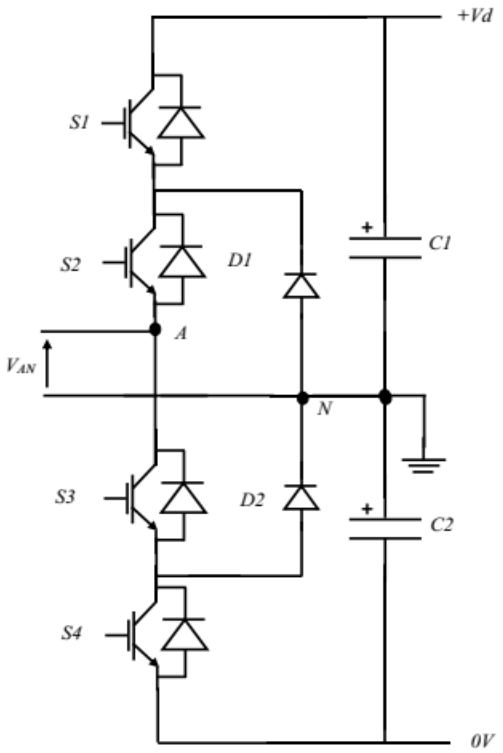

Fig. 2. A leg of a 3 level NPC converter.

An open loop simulation of the upper stage of the converter using a sinusoidal PWM controller is carried out, with a resistive load $R = 1k\Omega$. The simulation is first done for *Ls = 100µH;* then for *Ls = 1mH*. Results of simulations are presented in Fig.4 and Fig.5 respectively.

For $L_S = 100\mu H$, the phase shift between the primary voltage and the secondary voltage is not perceptible. For very small values of the inductance *Ls*, the power transfer between the two sides of the isolated converter is therefore negligible, it can also be noticed the voltages *V1* and *V2* are almost in phase (**Fig.6**).

Table 2. Steady state operation of the converter.

	$[t_0; t_1]$	$[t_1; t_1 + DT_s]$	$[t_1 + DT_s; t_2]$	$[t_2; t_2 + DT_s]$
$S_1;S_4$	1	1	0	0
$S_2;S_3$	0	0	1	1
$S_{51};S_{52}$	1	0	0	1
$S_{61};S_{62}$	0	1	1	0
$S_{71};S_{72}$	0	1	1	0
$S_{81};S_{82}$	1	0	0	1
V_1	V1	V1	0	V1
V_2	0	mV1	mV1	0
I_L	increase	increase	decrease	decrease

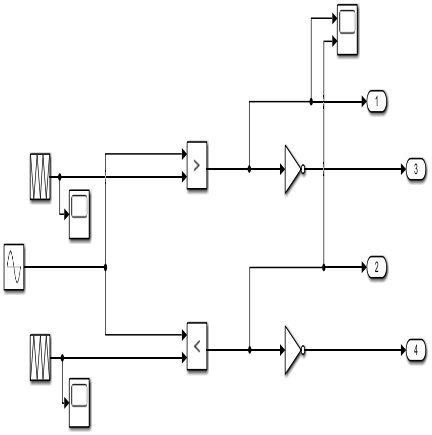

Fig. 3. Simulink model of the sinusoidal PWM.

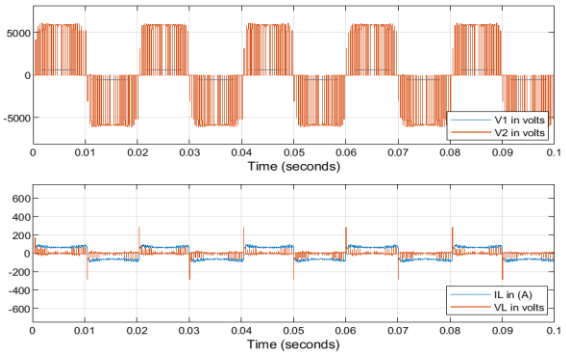

Fig. 4. Open loop simulation of the upper stage of the converter: Ls = 100µF, R = 1KΩ.

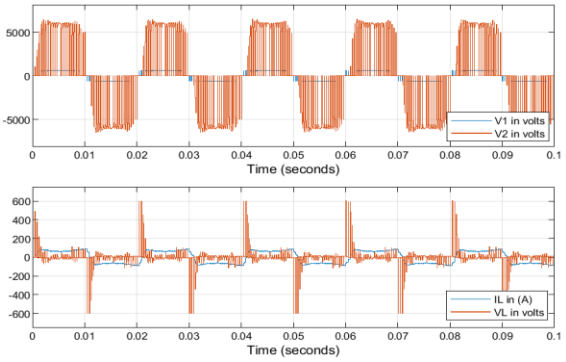

Fig. 5. Open loop simulation of the upper stage of the converter: Ls = 1mH, R = 1kΩ.

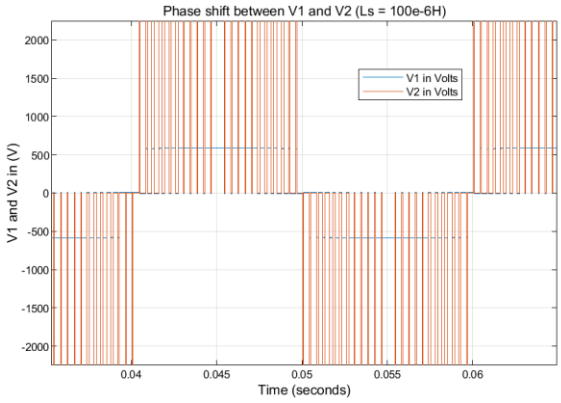

Fig. 6. Phase shift between V1 and V2 for Ls =100µH.

For *Ls = 1mH*, the phase shift between *V1* and *V2* is very well perceptible. The power transfer between both sides of the converter is therefore more important. There is a phase shift between *V1* and *V2* (Fig.7).

III. PROPOSED CONTROL SCHEME

The proposed control scheme is a combination of sliding mode control and direct power control which we can call sliding mode direct power control. The neutral point voltage balance is achieved using a simple auxiliary inductive circuit.

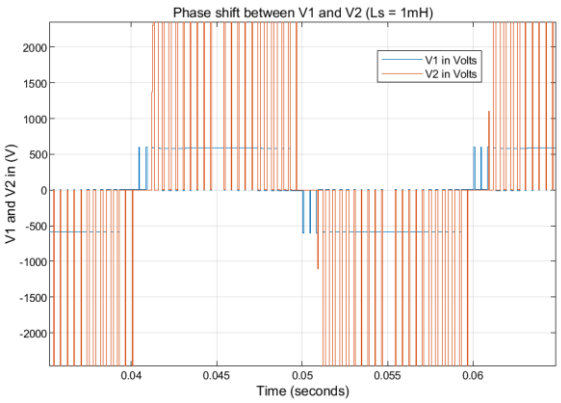

Fig. 7. Phase shift between *V1* and *V2* for *Ls* = 1mH

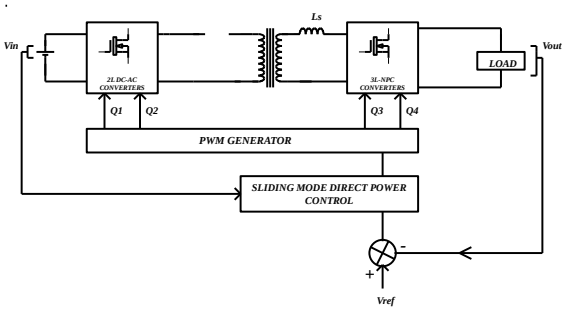

Fig. 8. Schematic diagram of the proposed sliding mode direct power control scheme.

Table 3. PWM outputs with corresponding controlled switches

Q1	S_1. S_4
Q2	S_2; S_3
Q3	S_{51};S_{52}; S_{81};S_{82}
Q4	S_{61};S_{62} S_{71};S_{72}

3.1. Sliding mode direct power control of the converter

The authors of [12] used a similar technique for the voltage control of a dual active bridge converter. The controller calculates the suitable duty ratio *D* that will enable the converter to track the output voltage reference *Vref*. The predetermined sliding mode surface *S* is fundamentally defined by

the error combination between the output voltage *Vout* and its reference value *Vref*.

$$S = \alpha_1(V_{ref} - V_{out}) + \alpha_2 \int_0^t (V_{ref} - V_{out}) \quad (4)$$

$$\frac{dS}{dt} = -\alpha_1 \dot{V_{out}} + \alpha_2(V_{ref} - V_{out}) \quad (5)$$

α_1 and α_2 are the sliding surface coefficients. At steady state, $\frac{dS}{dt} = 0$ and $S = 0$, which satisfies the existence condition of the sliding mode control. Moreover, the existence of both proportional and integral coefficients gives a flexibility to adjust the loop bandwidth [13]. Let i_C the current flowing in the capacitive branch of the converter i_C can be written as follows:

$$i_C = C\frac{dV_{out}}{dt} = I_{Ls} - I_o \quad (6)$$

Where *C* is the total capacitance, I_{LS} is the current in the inductance *Ls* and *Io* is the load current. From (6) we can deduce the following:

$$\frac{dV_{out}}{dt} = \dot{V_{out}} = \frac{I_{Ls} - I_o}{C} = \frac{I_{Ls}}{C} - \frac{V_{out}}{CR} + \frac{D(1-D)V_{in}}{4fCL_S} \quad (7)$$

With

$$I_{Ls} = \frac{(-2D+1)V_{in} - V_{out}}{2R} \quad (8)$$

The equilibrium phase shifted ratio *D* is determined by plugging (7) into (5). By solving the quadratic equation obtained with respect to *D*, we have:

$$D = \frac{1 - \frac{4fLs}{R} + \sqrt{\left(\frac{4fLs}{R} - 1\right)^2 - 8fLs + \frac{3V_{out}}{V_{in}R} + \frac{2C\alpha_2}{V_{in}\alpha_1}(V_{ref\_}Vout)}}{2} \quad (9)$$

D is the positive solution out of the two solutions arrived at. The settling time is tuned based on the selection of the sliding surface coefficients α_1 and α_2. So, these coefficients are chosen such as to have the best settling time for the output voltage *Vout*.

3.2. Neutral point voltage balancing technique

For the balancing of the neutral point voltage, we use a simple inductive auxiliary circuit. The circuit is made of two switches with an inductor. The inductor enables energy transfer from the capacitor having the highest voltage to the next one having a smaller voltage across its terminals. The inductance is chosen so as to enable a continuous flow of current in the inductor [14]. Fig. 9 below is an illustration of the circuit and Fig. 10 is the Simulink implementation of the control of switches S_A and S_B. T12 controls S_A and T34 controls S_B. L = 100µ*H*

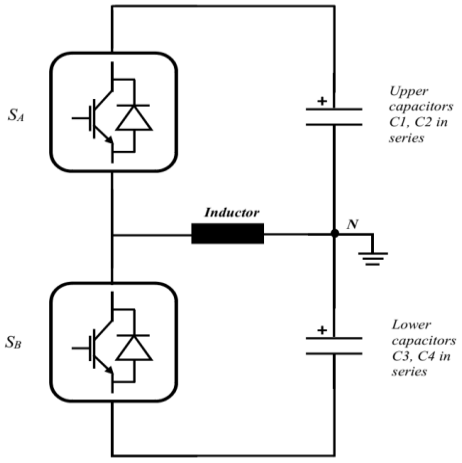

Fig. 9. Neutral point voltage balancing technique.

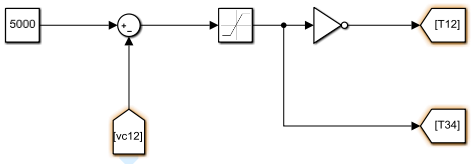

Fig. 10. Control of switches S_A and S_B.

IV. SIMULATIONS AND DISCUSSIONS

Simulation parameters are given in Table 4 below.

Table 4. Simulation parameters

Parameters	***Values***
Vin	*600V(Boost mode)* *10kV(Buck mode)*
Ls	*100µH*
Transformation ratio m	*10*
Frequency f	*100kHz*
$C_1=C_2=C_3=C_4$	*1000µF*
R	*300Ω (HV mode) et 1kΩ (LV mode)*
C_o	*25000µF*

4.1. Output voltage reference tracking in HV Mode

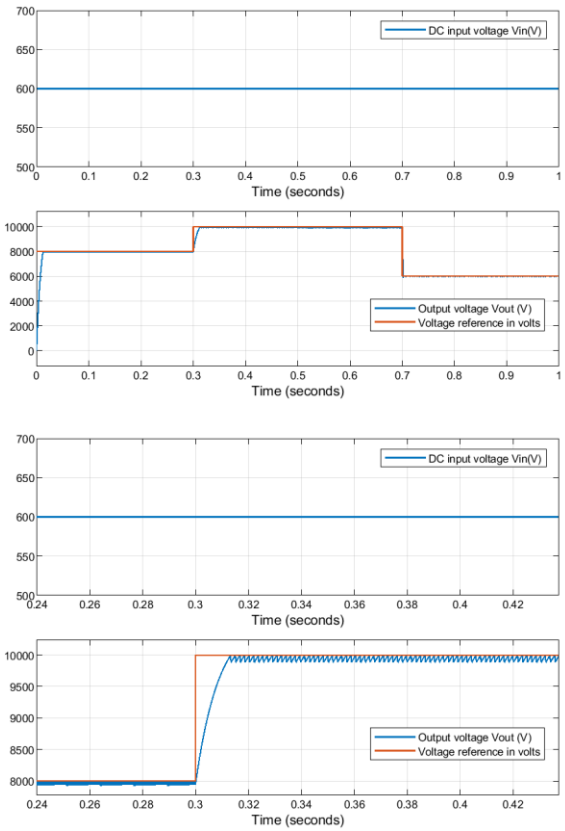

Fig. 11. Output Voltage reference tracking in HV mode.

There is a good tracking of the reference by the output voltage. It can be observed that, in tracking the reference, the output voltage moves from 8kV to 10kV and down to 6kV with a good accuracy. The DC input voltage source is maintained at 600V.

4.2. Output voltage reference tracking in LV mode

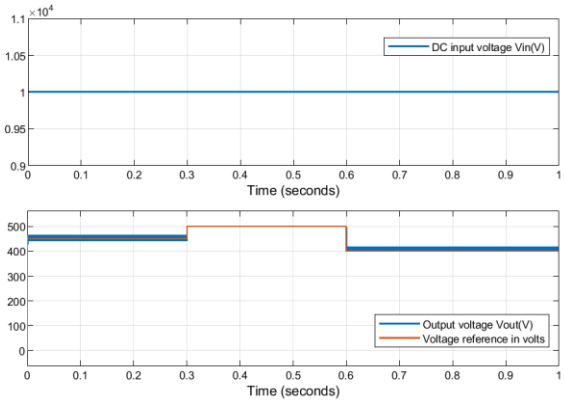

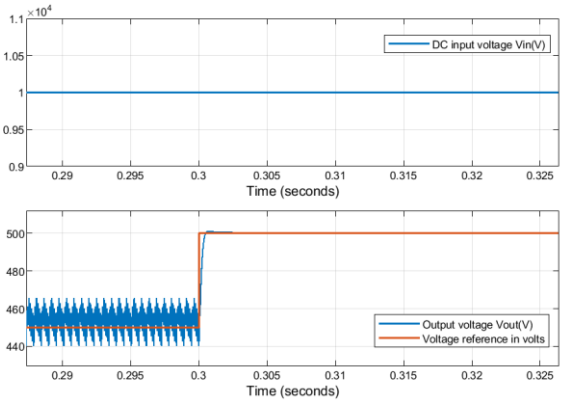

Fig. 12. Output Voltage reference tracking, Buck mode.

The HV DC input is kept at 10kV. The output voltage tracks the reference from 450 V to 500V and down to 400V, with a good accuracy.

4.3. Load variation

The load is varied in order to assess the robustness of the controller in HV mode as well as in LV mode.

4.3.1. HV mode

Resistive loads of 2kΩ each are successively added in parallel to the initial 300Ω load resistor at the instants 0.3s and 0.7s respectively. It can be observed that, despite the changes in load, the output voltage *Vout* remains at the set reference of 8kV. (Fig.11)

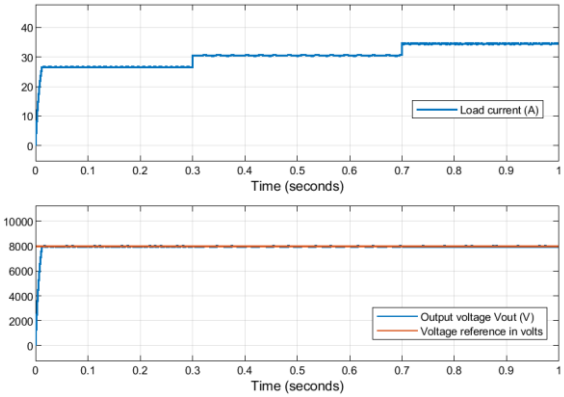

Fig. 13. Load variation, HV mode.

4.3.2. LV mode

Resistive loads of 10kΩ each are successively added in parallel to the initial 1kΩ load resistor, at the instants 0.3s and 0.7s respectively. It can be observed that, despite the changes in load, the output voltage *Vout* remains at the set reference of 400V (Fig.12).

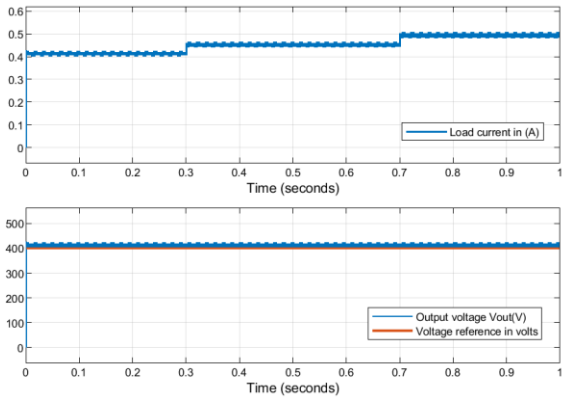

Fig. 14. Load variation, LV mode

4.4. Neutral point voltage balancing

The output voltage is set at 10kV, the simulation is run for 10s. It can be observed that the neutral point voltage *Vn* varies between $4*10^{-8}$V and $8*10^{-8}$V approximately, as the output voltage remains at the set value of 10kV; and this voltage is not diverging. This exhibits a good neutral point voltage balancing given the very small value of *Vn* and the little variation it presents over a long duration of simulation (Fig.15).

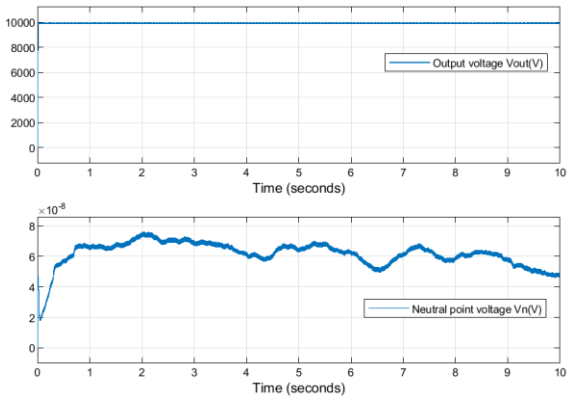

Fig. 15. Neutral point voltage balancing.

V. CONCLUSION

This paper proposes a sliding mode direct power control of a DC-DC bidirectional converter destined for high voltage applications. The control scheme presents the following advantages: good robustness manifested through an accurate output voltage reference tracking. Moreover, it has a fast response and is easy to implement. The HV capability of the DC-DC converter investigated makes it suitable for HVDC transmission systems and high voltage DC motor drives. Further works may consist in improving on the neutral point voltage balancing technique, and also in reducing the rising time of the output voltage when the converter is working in HV mode.

REFERENCES

[1] J. S. Manguelle, Convertisseurs Multiniveaux Asymétriques Alimentés par transformateurs Multi-secondaires Basse Fréquence : Réactions au réseau d'alimentation, doctoral thesis, EPFL, 2004.

[2] Tao Zhou , Zeliang Shu, Hongjian Lin , Deng Luo , Yajun Chen and Xiaoxiao Guo, A High-Power-Density Single-Phase Rectifier Based on Three-Level Neutral-Point Clamped Circuits, MDPI ,Energies , 10, 697, 2017.

[3] J. D. Gomez Palomino, Design and Evaluation of a Single Phase 5 Level Full Bridge Neutral Point Clamped Multi Level Converter, doctoral thesis, The university of Sheffield, 2017.

[4] A. Calle, J. Rocabert, S. Busquets-Monge, J. Bordonau, S. Alepuz, J. Peracaula ,Three-Level Three-Phase Neutral-Point-Clamped Back-to-Back Converter Applied to a Wind Emulator", Universitat Politecnica de Catalunya.

[5] A. L. Fuerback A. J. Perin M. L. Heldwein, C. S. Postiglione, Single-Phase/-Stage NPC-Based Rectifier Integrating a Simple DCM PFC Technique, Conference paper, EPE'13 ECCE Europe ISBN: 978-90-75815-17-7 and 978-1-4799-0114-2, 2013.

[6] Eun-Su Jun and Sangshin Kwak ,A Highly Efficient Single-Phase Three-Level Neutral Point Clamped (NPC) Converter Based on Predictive Control with Reduced Number of Commutations, MDPI Energies, 11, 3524, 2018; doi:10.3390/en11123524

[7] Eun-Su Jun, Minh Hoang Nguyen and Sangshin Kwak, Model Predictive Control Method Based on Deterministic Reference Voltage for Single-Phase Three-Level NPC Converters, MDPI Appl. Sci. 2020, 10, 8840; doi:10.3390/app10248840

[8] Chang-Liang Xia, Zhe Xu, and Jia-Xin Zhao, A New Direct Power Control Strategy for NPC Three-Level Voltage Source Rectifiers Using a Novel Vector Influence Table Method, Journal of Power Electronics, Vol. 15, No. 1, pp. 106-115, January 2015.

[9] Pekik Argo Dahono and Een Taryana, A New Voltage Control Method for Single-Phase PWM Inverters, ITB Journal of Engineering Science, August 2011.

[10] Saman A. Gorji, Hosein G. Sahebi, Mehran Ektesabi, and Ahmad B. Rad, Topologies and

Control Schemes of Bidirectional DC–DC Power Converters: An Overview, IEEE, Volume7, 2019, IEEE DOI:10.1109/ACCESS.2019.2937239.

[11] Muhammad H. Rashid et al., Power Electronics Handbook: Devices, Circuits, and Applications.", Third Edition, Elsevier, 2011, 1409 pages.

[12] Shenli Zou, Sheng Zheng, Madhu Chinthavali, Design, Analyses and Validation of Sliding Mode Control for a DAB DC-DC Converter, UT-Battelle, LLC, under contract DE-AC05-00OR22725 with the US Department of Energy (DOE), http://energy.gov/downloads/ doe-public-access-plan.

[13] S. Zou, A. Mallik, J. Lu, and A. Khaligh, Sliding Mode Control Scheme for a CLLC Resonant Converter, IEEE Transactions on Power Electronics, 2019. doi: 10.1109/TPEL.2019.2904456

[14] A. Leredde, Etude, commande et mise en œuvre de nouvelles structures multiniveaux, doctoral thesis, INPT, 2011.